Systematic Assay of the Influence of Current Ripples on Polymer Electrolyte Membrane(s) in Low-Temperature Fuel Cells

M. Stark, G. Krost, S. Gössling, P. Beckhaus

This document appeared in

Detlef Stolten, Thomas Grube (Eds.):
18th World Hydrogen Energy Conference 2010 - WHEC 2010
Parallel Sessions Book 1: Fuel Cell Basics / Fuel Infrastructures
Proceedings of the WHEC, May 16.-21. 2010, Essen
Schriften des Forschungszentrums Jülich / Energy & Environment, Vol. 78-1
Institute of Energy Research - Fuel Cells (IEF-3)
Forschungszentrum Jülich GmbH, Zentralbibliothek, Verlag, 2010
ISBN: 978-3-89336-651-4

Systematic Assay of the Influence of Current Ripples on Polymer Electrolyte Membrane(s) in Low-Temperature Fuel Cells

M. Stark, **G. Krost**, University Duisburg-Essen, Germany
S. Gössling, **P. Beckhaus**, ZBT- Duisburg, Germany

1 Introduction

The non-linear characteristics of inverters used for feeding the electrical direct current (DC) output of fuel cells into the public alternating current (AC) based grid leads to the occurrence of current ripples both on AC and DC sides. The DC current ripples are suspected of having degrading effects on the fuel cell, which is usually counteracted by an anticipation to install filter circuits. Rather, a comprehensive analysis of coherences is still missing. On the other hand, deeper insight and authoritative evidence would allow for creating plain specifications for inverter manufacturers and fuel cell operators. The challenge of the reported project was to systematically investigate the influence of current ripples of various frequencies and amplitudes on PEM cells by long term observation and comparison with a reference cell loaded by pure DC. For the occurrence of ripples in commonly used pulse width modulation based inverters three different mechanisms are responsible:

a) Harmonics of predominantly second order result from modulation DC / grid frequency.

b) The usual inverter's switching clock frequencies are in the range of several kHz.

c) Natural frequencies of inverter circuitry, triggered by switching of transistors, are in the MHz range.

2 Test Rig for Long Term Tests

For the investigations a specific test rig was configured, allowing for simultaneous operation of three identical PEM fuel cell stacks under distinct ripple conditions.

2.1 Fuel cell stacks

The fuel cell stacks used for the different tests are composed of injection molded bipolar plates consisting of PP, carbon black and graphite, between which the membrane electrode assemble (MEA) and the appertaining seal is clamped. Bipolar plates, MEA and seals of the stacks were selected to be part of one and the same manufacturing charge in order to minimize variance. The bipolar plates are identical at both anode and cathode sides and contain a meander flow field with an active area of 50 cm^2. For cooling purposes, at the back side of the bipolar plates a second flow field is arranged in which tempered water is circulated in order to gain a homogeneously dispersed temperature across the whole cell.

2.2 Media supply

Provisioning of three PEM stacks operated in parallel with gases is shown in Figure 1. Cathode air as well as de-mineralized water needed for air humidification are supplied by mass flow controllers; the mixture is overheated in an evaporator for complete vaporization. The segment of the feeding line to the fuel cell is heated to avoid water re-condensation. At the anodic side of the fuel cell the unused hydrogen is re-circulated, which is a general practice and provides test conditions close to real supply systems. Pressure-reduced fresh hydrogen is mixed with re-circulated anode gas before re-supply to the stack; due to the re-circulation a high stoichiometry at the anode is achieved. The complete re-circulation circuit as well as the fresh hydrogen are heated to avoid water condensation. The surplus of water in the circuit is removed by a dehydrator. The high partial pressure of nitrogen at the cathode side of the fuel cell effects diffusion of nitrogen through the MEA to the anode side; the closed gas circuit at the anode side leads to increasing concentration of nitrogen. To keep the concentration of nitrogen in the anode circuit low, it is frequently purged by a valve. The cell temperature is controlled by tempered de-mineralized water flow; the conductivity of the water is steadily surveyed, and the water is changed when necessary.

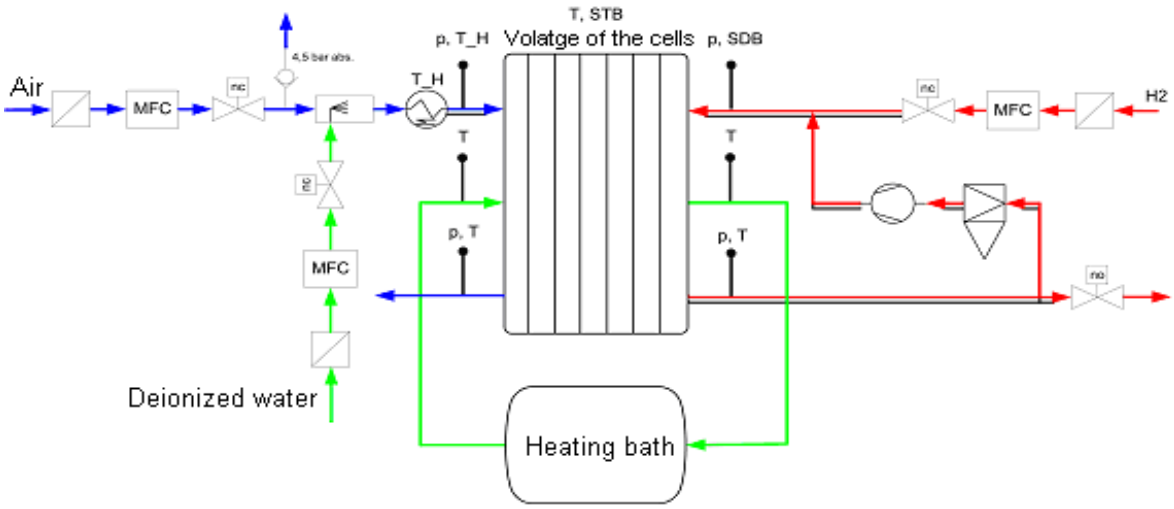

Figure 1: Media supply of test rig (one channel shown).

2.3 Electronic load

The electronic load was particularly assembled for the tests. It consists of three identical, independently controlled circuits based on power transistors (MOS FET types) used as controllable resistors, as well as appertaining control and monitoring circuits, Figure 2.

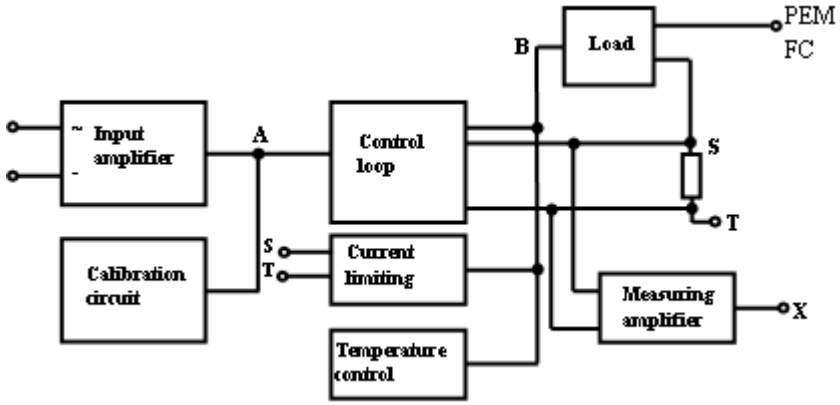

Figure 2: Block diagram of the electronic load (one channel shown).

The input signal, representing the aspired fuel cell load current, is composed by summing up the basic DC and superimposed AC constituents, and then amplified. A calibration circuit allows for adjusting the input signals or, alternatively, those of an external analogue output board for instance. The control loop, receiving the input signal from the input amplifier, actuates the power MOS FET. The actual current in the load circuit is measured by voltage drop at the shunt, followed by a measuring amplifier, which can be calibrated internally. To avoid thermal overload a temperature control was established; furthermore, a current limiting circuit cares for fault protection.

3 Measurement Methods

Terminal voltages and load currents of the stacks under investigation were steadily recorded during the long term tests. For more detailed characterization of the stack conditions, three commonly used methods for in-situ characterization of fuel cells have been applied in certain time intervals: To achieve a quick survey of the stationary behavior, the polarization curve is a well proven method. The electrochemical impedance spectroscopy (EIS) as well as the current interrupt method (CI) provide information about the frequency dependant behavior, [1], [2], [3].

4 Experimental Results of the Long Term Tests

For the first long term experiment – lasting 600 h – two 5-cell fuel cell stacks were used only. The electric parameters of the experiment are given in Table 1.

Table 1: Parameters of first long term experiment.

	DC current	AC current	Frequency
Stack 1	40 A	8 A (20%)	100 Hz
Stack 2	40 A	0 A	- (pure DC)

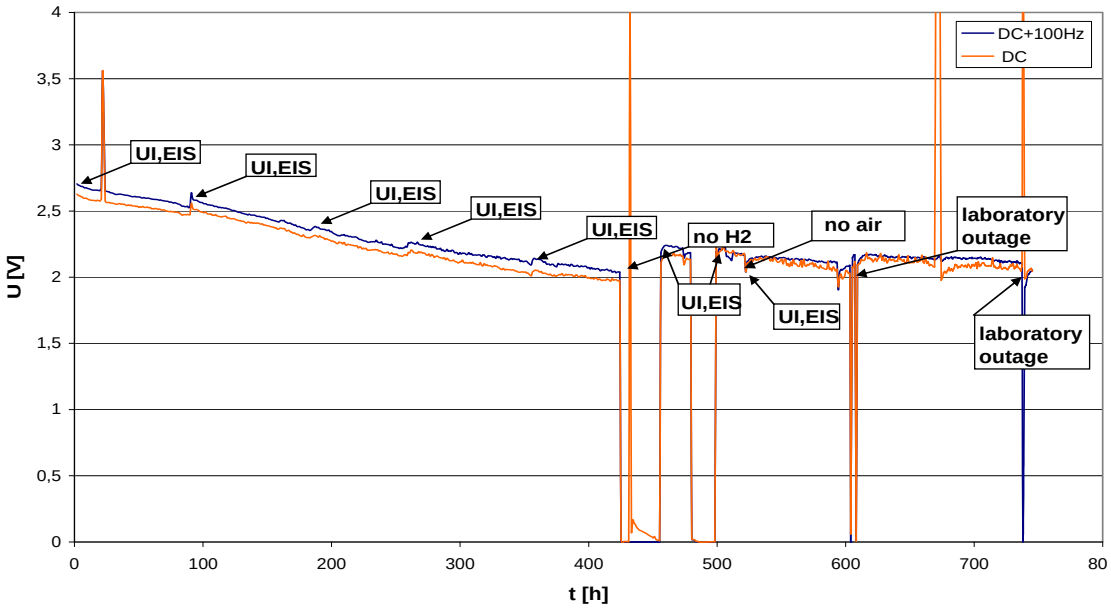

Figure 3: First long term experiment: terminal voltages of investigated stacks over time.

With 40 A basic DC current the active membrane surface of 50 cm^2 was loaded by 800 mA/cm^2 which is relatively high; the amplitude of the second harmonic (100 Hz for grid frequency of 50 Hz) at 20 % of DC was consciously chosen rather high too, in order to provoke a noticeable ripple effect on the fuel cell stack. Both terminal voltages and loading currents were recorded every 5 s, polarization curves as well as EIS curves in the frequency range 0 … 20 kHz were taken two times per week. Figure 3 shows the stack terminal voltages (5 cells) over time for the complete runtime of the experiment; for the stack exposed to ripples the RMS values, for the reference stack the average values are entered.

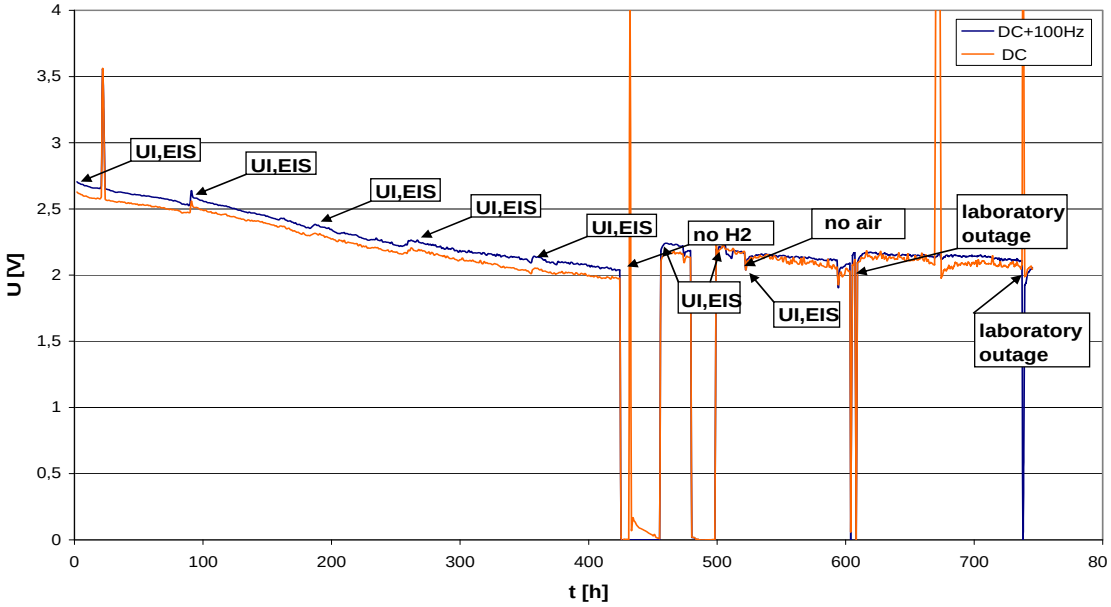

Figure 3: First long term experiment: terminal voltages of investigated stacks over time.

A significant degradation of 300 µV/h per cell on average can be observed which could be reduced to approximately 100 µV/h per cell after several interruptions of lab operation; the experiment was stopped when average cell voltages of 400 mV were reached. The appertaining polarization curves of the two stacks at the beginning and end of the experiment are shown in Figure 4.

The characteristics of the stack exposed to ripple is rather identical to that of the one loaded by pure DC (low divergence in the range of diffusion processes may be caused by slightly different temperature, humidity or load currents); obviously no noticeable impact of ripple on the static behavior of the stack can be recognized.

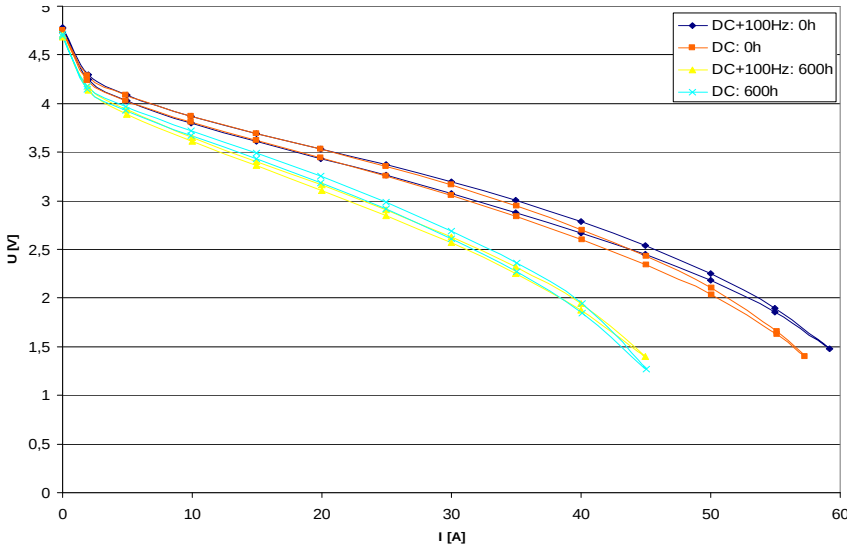

Figure 4: Polarization curves of stacks at begin and end of first long term test.

The EIS curves in Figure 5, taken at start and end of the experiment, also show the degradation over time of both stacks, in particular at the cathode bow (low frequencies). For higher frequencies the curves are approaching to each other which doesn't give any hint of ripple impact as well. After implementation of several improvements at the test rig a second long term experiment was started, investigating three identical new stacks. As a consequence of the unnoticeable ripple impact in the first experiment the basic DC load was reduced to 20 A, connected with significant increments of ripple amplitudes up to 15 A corresponding to a remarkable 75 % of basic DC. Ripple frequencies were chosen at 100 Hz and 20 kHz this time. The electric parameters are summarized in Table 2.

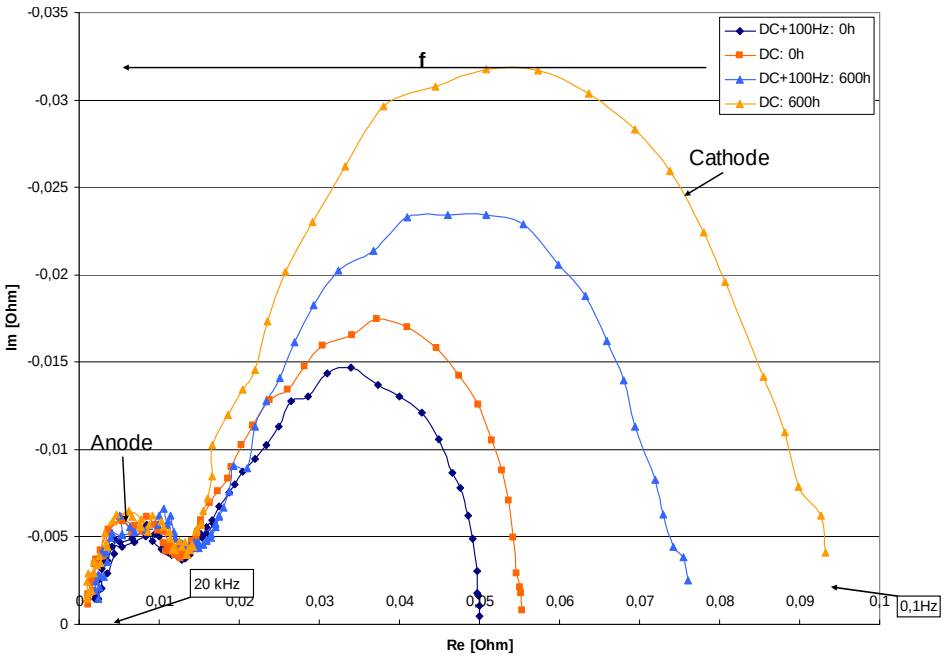

Figure 5: EIS curves of stacks at begin and end of first long term test.

The measurements were recorded just like in the first experiment, except the polarization curve which was taken every two weeks only in order to diminish the impact on steady operation (the effect of EIS measurements taken at very low currents is much lower). The total duration of this experiment was 2280 h. The consequence of several improvements at the test rig (supply of gases) was that the terminal voltage degraded much more moderately, but during this experiment several outages of lab and test rig operation happened too; the operation interruptions led to temporary recovery of the stack voltages, Figure 6.

Table 2: Parameters of second long term experiment.

	DC current	AC current	Frequency
Stack 1	20 A	0 A (0%)	- (pure DC)
Stack 2	20 A	15 A (75%)	100 Hz
Stack 3	20 A	15 A (75%)	20 kHz

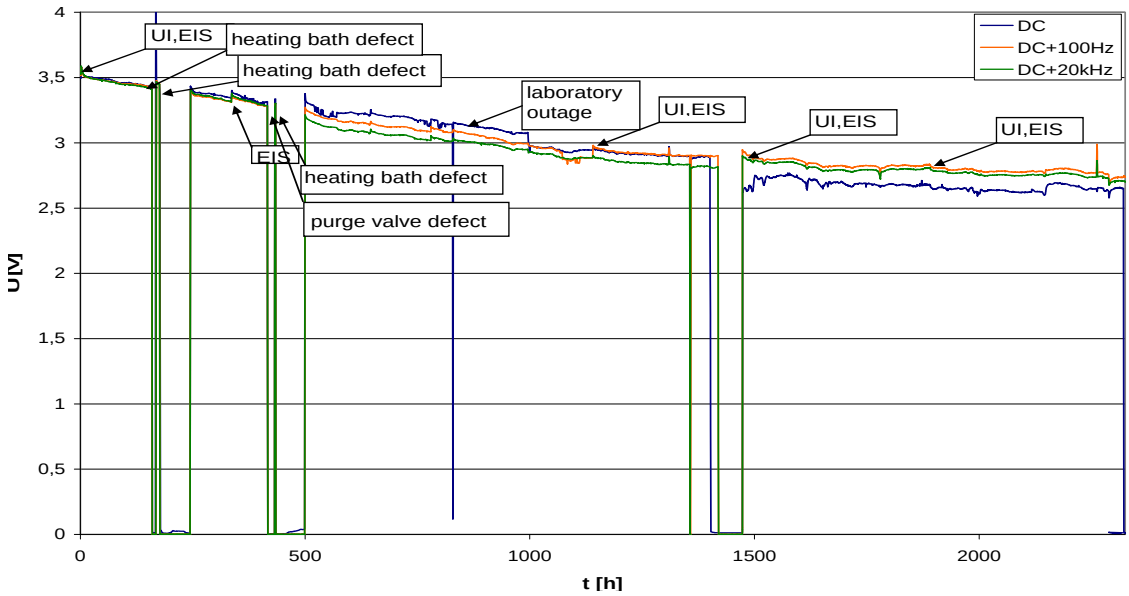

Figure 6: Second long term experiment: terminal voltages of investigated 5 cell stacks over time.

The polarization and EIS curves of the three stacks investigated, again, do not differ significantly, Figure 7 and Figure 8. The moderate distinguishable deviation of the reference stack (not impacted by ripples) could later be attributed to single cells of this particular stack, for which some drains were congested by metallic deposits. Obviously the second experiment, conducted under extreme ripple conditions, could not produce any observable impact of ripples on stack performance too.

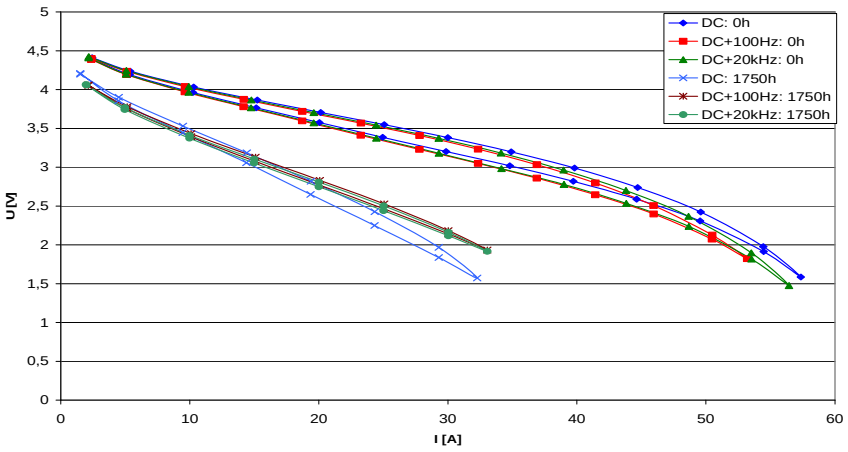

Figure 7: Polarization curves of 5 cell stacks at begin and end of second long term test.

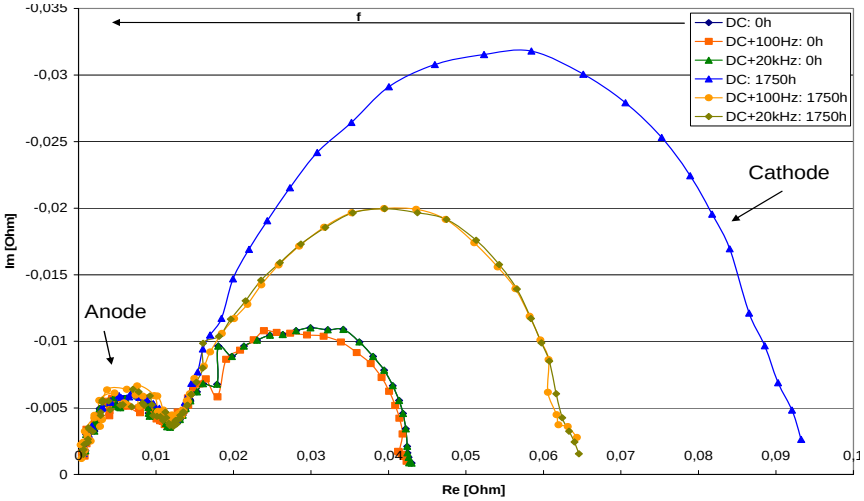

Figure 8: EIS curves of stacks at begin and end of first long term test.

In searching for further influences, stoichiometry was identified as another possible factor. For this reason in the frame of a third experiment the general stoichiometry was reduced to a value of 1.7; this should theoretically lead to short transitory undersupply (at stoichiometry of 0.97 only) during the ripple amplitude maxima. The parameters applied to this experiment, lasting 1750 h, are summarized in Table 3.

Table 3: Parameters of third long term experiment.

	DC current	AC current	Frequency
Stack 1	20 A	0 A (0%)	- (pure DC)
Stack 2	20 A	15 A (75%)	100 Hz
Stack 3	20 A	7.5 A (37.5%)	20 kHz

	Humidity	Stoichiometry
Cathode	average: 61.5% @ 74°C input: 36%, output: 85%	1.7
Anode	70% (100% @ 66°C)	-

While the general degradation over time of all stacks has very much improved in this case (Figure 9), the polarization and EIS curves (not specifically shown in this case) appeared unremarkable again with regard to ripple influences, i.e. no significant differences between ripple-loaded and reference (pure DC) stacks could be identified also in this case.

In summary for the three long term experiments the following can be stated:

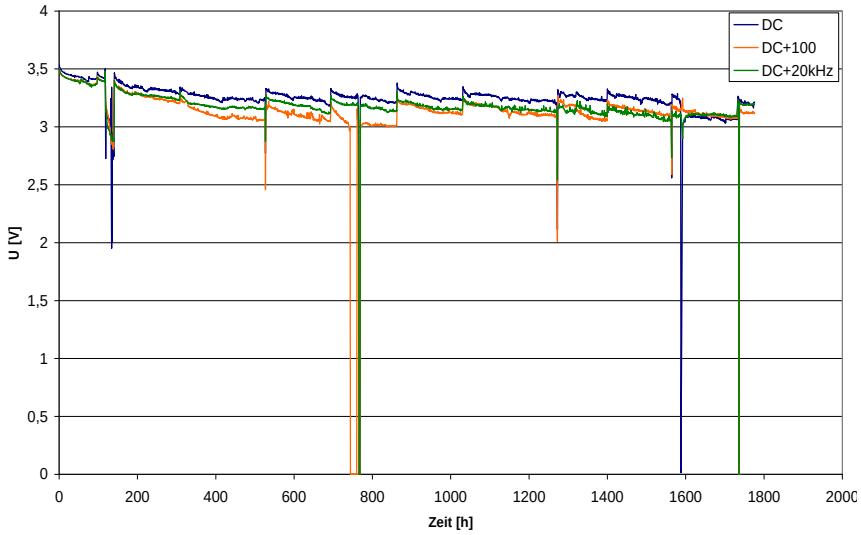

Figure 10: Third long term test: terminal voltages of investigated 5 cell stacks.

the test rig conditions could steadily be improved, finally achieving a general (not ripple-caused) cell degradation in the typical range commonly known from various literature; an impact of ripples on long term cell performance could, even in the case of extraordinary ripple amplitudes, not be observed.

5 Further Experiments

As shown in [4], current ripples have diminishing impact on the electric output power of fuel cells. This effect was further investigated in the present study by variation of ripple amplitudes at different operating points of a two-cell stack. The first experiment was conducted at 20 A DC load; ripple amplitudes of 0.1 A, 0.5 A, 1 A, 2 A, 5 A and 10 A were superimposed at frequencies of 10 Hz, 100 Hz and 1 kHz. Measurements of stack output power were taken when a stable operation point arose. The electrical output power of the stack depending on ripple amplitudes – which were set in rising order in this case – at the given frequencies is shown in Figure 10. It is conspicuous that besides the power decrement at increasing ripple amplitudes – known from, and explained by additional cell resistance in, [4] – a local power minimum occurs at very low amplitudes for all frequencies investigated. In alleviated form this phenomenon can also be observed at a lower DC operating point of 10 A, but there is no plausible explanation so far.

6 Conclusion

The influence of current ripples on long term degradation of PEM fuel cells was systematically investigated. Test stacks were exposed to synthetic current ripples of various frequencies and extraordinary amplitudes for longer time intervals. In summary it can be stated that hints to an impact of current ripples on long term degradation of stacks could not be identified. In consequence, demands to inverter manufacturers to care for strict limitation of ripples in fuel cell circuits could be re-assessed, thus sparing cost and losses of filters.

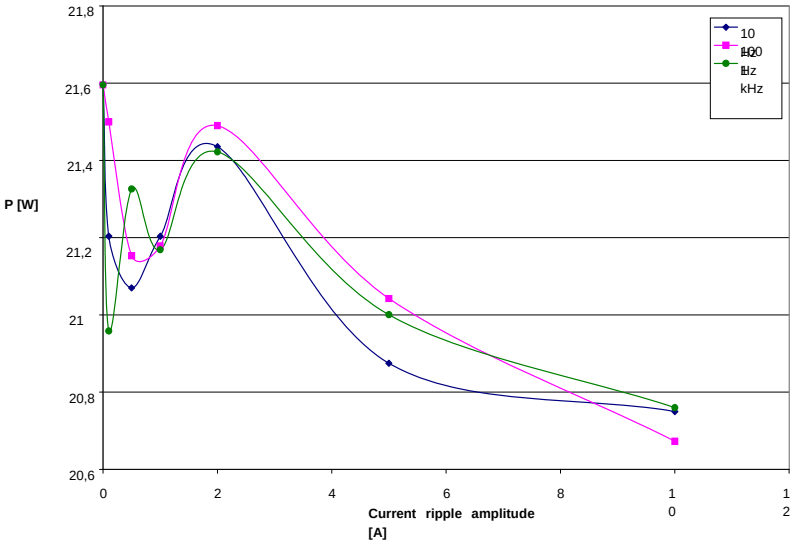

Figure 10: Stack output power depending on amplitudes of ripples at different frequencies.

Acknowledgement

Thanks to “Zentralverband Elektrotechnik- und Elektronikindustrie e.V..“(ZVEI)„“for sponsoring this project (15279 N) with allocated funds from “Bundesministerium für Wirtschaft und Technologie (BMWi)“ through „Arbeitsgemeinschaft industrieller Forschungsvereinigungen "Otto-von-Guericke" e.V. (AiF)“.

References

[1] H. Kuhn, Charakterisierung von Polymer-Elektrolyt Brennstoffzellen mittels Elektrochemischer Impedanzspektroskopie; Dissertation; University Karlsruhe, Germany, 2006.

[2] D. Vladikova, The technique of the differential impedance analysis: Part I: Basics of the impedance spectroscopy; Proceedings of the International Workshop “Advanced Techniques for Energy Sources Investigation and Testing”, 2004, Sofia, Bulgaria.

[3] B. Andreaus, Die Polymer-Elektrolyt Brennstoffzelle – Charakterisierung ausgewählter Phänomene durch elektrochemische Impedanzspektroskopie; Dissertation, École Polytechnique Fédérale de Lausanne, Switzerland, 2002.

[4] Schindele, Einsatz eines leistungselektronischen Stellglieds zur Parameteridentifikation und optimalen Betriebsführung von PEM-Brennstoffzellensystemen; Dissertation, University Karlsruhe, Germany, 2006.